Int. J. Electrochem. Sci., 10 **(2015)** 838 - 847

International Journal of
ELECTROCHEMICAL
SCIENCE
www.electrochemsci.org

Synthesis and Characterization of $Li(Li_{0.2}Mn_{0.4}Fe_{0.2}M_{0.2})O_2$ (M=Co, Ni, Cr, Al) Cathode Materials for Li-ion Batteries

Jiangang Li[1,*], *Jiuhua Chen*[1], *Jianjun Li*[2,3], *Lei Wang*[a], *Li Wang*[2,4], *Xiangming He*[2,4,*]

[1] Beijing Institute of Petrochemical Technology, Beijing 102617, China
[2] Institute of Nuclear & New Energy Technology, Tsinghua University, Beijing 100084, China
[3] Huadong Institute of Lithium Ion Battery, Zhangjiagang, Jiangsu 215600, China
[4] State Key Laboratory of Automotive Safety and Energy, Tsinghua University, Beijing 100084
[*]E-mail: hexm@tsinghua.edu.cn; lijiangang@bipt.edu.cn

Received: 26 October 2014 / *Accepted:* 24 November 2014 / *Published:* 2 December 2014

$Li(Li_{0.2}Mn_{0.4}Fe_{0.2}M_{0.2})O_2$ (M=Co, Ni, Cr, Al) cathode materials were prepared by citric acid assisted sol-gel process, and the effects of ion-doping on the structural and electrochemical properties of as-prepared materials were investigated. The results show that both Co- and Ni- doped samples with pure layered α-$NaFeO_2$ phase are easily prepared, Al-doped sample can only be obtained while annealed at 600 ^oC ~700 ^oC, but Cr-doped samples always contain impure phase of Li_2CrO_4 and $LiFeO_2$. All of doped samples prepared at 700 ^oC exhibit the highest discharge capacity. Among them, Cr doping is not beneficial to electrochemical performance due to existence of impure phase of Li_2CrO_4 and $LiFeO_2$. The Al-doped sample show higher capacity than Cr-doped one, but the notable low voltage plateau is similar. In contrast, both Co- and Ni- doped samples deliver higher capacity and voltage plateau, better structural stability during cycling. The Ni-doped sample presents higher voltage plateau than Co-doped one due to better reduction of the phase transformation from layered structure to spinel-like structure, showing more promising in view of cost and toxicity. It provides an initial capacity of 210 $mAhg^{-1}$ and 86.3% capacity retention after 21 cycles. The electrochemical performance is expected to be further improved by Al- and Ni- co-doping in future.

Keywords: Lithium-ion batteries; cathode materials; $LiFeO_2$-Li_2MnO_3; doping

1. INTRODUCTION

In recent years, Ni- and Co- composited layered Li_2MnO_3-$LiMO_2$ (M = Ni, Co, $Ni_{1-x}Co_x$, $Ni_{0.5}Mn_{0.5}$, $Ni_{1/3}Co_{1/3}Mn_{1/3}$, $Mn_{0.5-y}Ni_{0.5-y}Co_{2y}$) materials with high capacity and low cost have been investigated thoroughly in order to fill the demands of Lithium-ion batteries for EV and HEV [1-11]. $LiFeO_2$-Li_2MnO_3 based solid solution have been developed by Tabuchi et al [12-17], which also

attracted more attention due to cheapness of iron and the appearance of the Fe^{3+}/Fe^{4+} redox voltage around 4V in the sample [12, 18]. The $Li_{1+x}(Fe_yMn_{1-y})_{1-x}O_2$ solid solution ($0.3 \le y \le 0.5$) prepared by using a three-step preparation method including coprecipitation–hydrothermal–calcinations presented high capacity of >220 $mAhg^{-1}$. However, the cycleability was poor due to the transformation of layered Li_2MnO_3 to spinel phase as well as the formation of inactive cubic $LiFeO_2$ phase. In order to improve the cycling stability, doping of $LiFeO_2$-Li_2MnO_3 was investigated by some research groups. Tabuchi et al adopted 5% Al, Ni and Co doping to suppress capacity degradation of $Li[Li_{0.2}Fe_{0.4}Mn_{0.4}]O_2$, but the capacity was too small (70~80 $mAhg^{-1}$) [13]. Ni doping were further studies thoroughly by Tabuchi [19] and other researchers [20-23]. The sample with same content of Mn and Ni, such as $Li_{1.2}(Mn_{0.32}Ni_{0.32}Fe_{0.16})O_2$, showed good cycleability but lower capacity (~160 $mAhg^{-1}$) [20]. The sample with same content of Fe and Ni, such as $Li_{1+x}[(Fe_{1/2}Ni_{1/2})_yMn_{1-y}]_{1-x}O_2$ (x=0.2, y=0.4~0.5) [19], $0.6Li_2MnO_3$–$0.4Li[Mn_{1/3}Ni_{1/3}Fe_{1/3}]O_2$ [21], generally delivered high capacity of more than 220 $mAhg^{-1}$ and ~80% capacity retention after 20 cycles. Liu et al. reported $Li_{1.2}Mn_{0.585}Ni_{0.185}Fe_{0.03}O_2$ with capacity of 261.6 $mAhg^{-1}$ at 0.1C-rate and a high capacity retention rate of 90.9% after 80 cycles [22], but Fe content in the doped sample was very low. Our research group also developed a new composition of $LiFeO_2$-Li_2MnO_3 based solid solution $Li(Li_{0.23}Mn_{0.47}Fe_{0.2}Ni_{0.1})O_2$, which showed high capacity of 277.4 $mAhg^{-1}$ and better cycling stability [23]. Recently, investigation of $LiFe_{1-x}Cr_xO_2 \cdot Li_2MnO_3$ was reported by Zhao et al. [24]. The sample with x=0.25 presented an initial capacity of 238.9 $mAhg^{-1}$ and very good cycling stability (226 $mAhg^{-1}$ after 50 cycles) over 1.5~4.8V voltage range. However, only an initial capacity of 144.1 $mAhg^{-1}$ was obtained when charge-discharged over 2.0~4.8V. Therefore, modification of $LiFeO_2$-Li_2MnO_3 based solid solution is still needed to be carried out thoroughly in order to improve the electrochemical properties that can exceed the combined advantages of the existing cathodes with high capacity and stable cycleability.

In this study, $Li(Li_{0.2}Mn_{0.4}Fe_{0.2}M_{0.2})O_2$ (M=Co，Ni，Cr，Al) cathode materials were prepared by our proposed new sol-gel process [23], the effect of ion-doping on the structural and electrochemical properties of as-prepared materials were investigated, and the doping ions was optimized. As mentioned before, Co, Ni, Cr and Al doping of $LiFeO_2$-Li_2MnO_3 have been reported in some literatures [13, 19-24], but preparation methods and composition of the doped samples are different among them, and comparison of the doped ions on the structural and electrochemical properties have also been reported seldom.

2. EXPERIMENTAL

The cathode materials $Li(Li_{0.2}Mn_{0.4}Fe_{0.2}M_{0.2})O_2$ (M=Co, Ni, Cr, Al) were synthesized by our proposed citric acid assisted sol-gel process [23].The transparent wet gel was prepared firstly by stirring and heating the solution containing stoichiometric quantities of $LiNO_3$, $Mn(NO_3)_2$, $Fe(NO_3)_3$, $Ni(NO_3)_2$, $Co(NO_3)_2$, $Cr(NO_3)_3$, $Al(NO_3)_3$ and citric acid (Citric aicid : Total metal amount = 1:1 by molar ratio) at 70 °C for 12 h. The wet gel was then spray-dried at the condition of inlet air temperature 180°C and outlet temperature 65 °C ~ 70 °C to form transparent yellow foam gel. The

dried gel was heated at 400 °C for 5 h, and then annealed at 600 °C ~ 800 °C for 12 h followed by retreatment at 600 °C for 10 h in oxygen atmosphere to obtain products.

XRD-7000 X-ray Diffractometer was used to characterize the structure of $Li(Li_{0.2}Mn_{0.4}Fe_{0.2}M_{0.2})O_2$ (M=Co, Ni, Cr, Al) powders. Morphologies of as-prepared samples were taken from a Philips Quanta-400 field emission scanning electron microscope (SEM). X-ray photoelectron spectroscopy (XPS) data were obtained using an ESCALab250 electron spectrometer from Thermo Scientific Corporation with monochromatic 150 W Al Kα radiation. The base pressure was about 6.5×10^{-10} mbar. The binding energies were referenced to the C1s line at 284.8 eV from alkyl or adventurous carbon.

The electrochemical characterization was performed using CR2032 coin cells. The cell consisted of a cathode with the composition of 86wt% active materials, 8wt% Super P carbon black, and 6wt% poly(vinylidenefluoride), and a lithium metal anode separated by a Celguard 2400 microporous film. All investigated cells featured cathode electrodes with 0.8 cm in diameter and an active area of 0.50 cm^2 respectively. The mass of active material in each cathode was about 5 mg. The electrolyte was 1 $molL^{-1}$ $LiPF_6$ /EC+DEC+DMC (1:1:1 by volume). The cells were assembled in an Etelux-Lab2000 glove box filled with pure argon. The charge-discharge tests were galvanostatically performed on LAND cell test system over 2.5~4.8 V at the current densities of 10 mAg^{-1}. Zahner Elektrik IM6 electrochemical work station was used for cyclic voltammetry (CV) tests over 2.0~4.8 V at a scan rate of 0.075 mVs^{-1}, and AC-impedance measurements over the frequency range from 100 KHz to 10 mHz with the amplitude of 5 mV.

3. RESULTS AND DISCUSSION

Fig.1 shows the XRD patterns of as-prepared $Li(Li_{0.2}Mn_{0.4}Fe_{0.2}M_{0.2})O_2$ (M=Co, Ni, Cr, Al) materials. It is obvious that pure α-$NaFeO_2$ phase structure forms even at 600 ^oC for Co- and Ni- doped samples. The weak peaks between 20° and 23° are considered to be attributed to the superlattice ordering of Li and Mn in the transition-metal layers of Li_2MnO_3 [25]. Further increasing annealing temperatures leads to sharpening of the diffraction peaks, increased $I_{(003)}/I_{(104)}$ ratio and enhanced splitting of double peaks of (006)/(012) and (018)/(110). It indicates that increase of annealing temperature is helpful for improving the crystallinity and 2D cation ordering of the samples. However, impure phase peaks corresponding to Li_2CrO_4 [26] and cubic α-$LiFeO_2$ exist for all Cr-doped samples, showing that Cr doping is disadvantage for formation of uniform Li_2MnO_3-$LiFeO_2$ based solid solution with α-$NaFeO_2$ structure. Li_2CrO_4 peaks drop off with increase of annealing temperatures. It may be attributed to the formation of amorphous glass state Li_2CrO_4 at high temperatures [26]. For Al-doped samples prepared at 600 ^oC -700 ^oC, pure α-$NaFeO_2$ phase can be observed. However, impure phase peaks corresponding to γ-$LiAlO_2$ (JCPDS no.38-1464) appear when the temperature is increased to above 750 ^oC, due to the fact that higher annealing temperature is not beneficial to formation of α-$LiAlO_2$ with similar structure to layered $LiMO_2$ (Ni, Co, $Ni_{0.5}Mn_{0.5}$ etc.) [27].

SEM images of $Li(Li_{0.2}Mn_{0.4}Fe_{0.2}M_{0.2})O_2$ (M=Co, Ni, Cr, Al) prepared at 700 ^oC are shown in Fig.2. It can be seen that the morphologies of Co-, Ni- and Al- doped samples are very similar, small

primary particles with size of 100~200 nm aggregate to form big secondary particles. Different from them, primary particles of Cr-doped sample are well crystallized, which may be related to the existence of Li_2CrO_4 with low melting point [26].

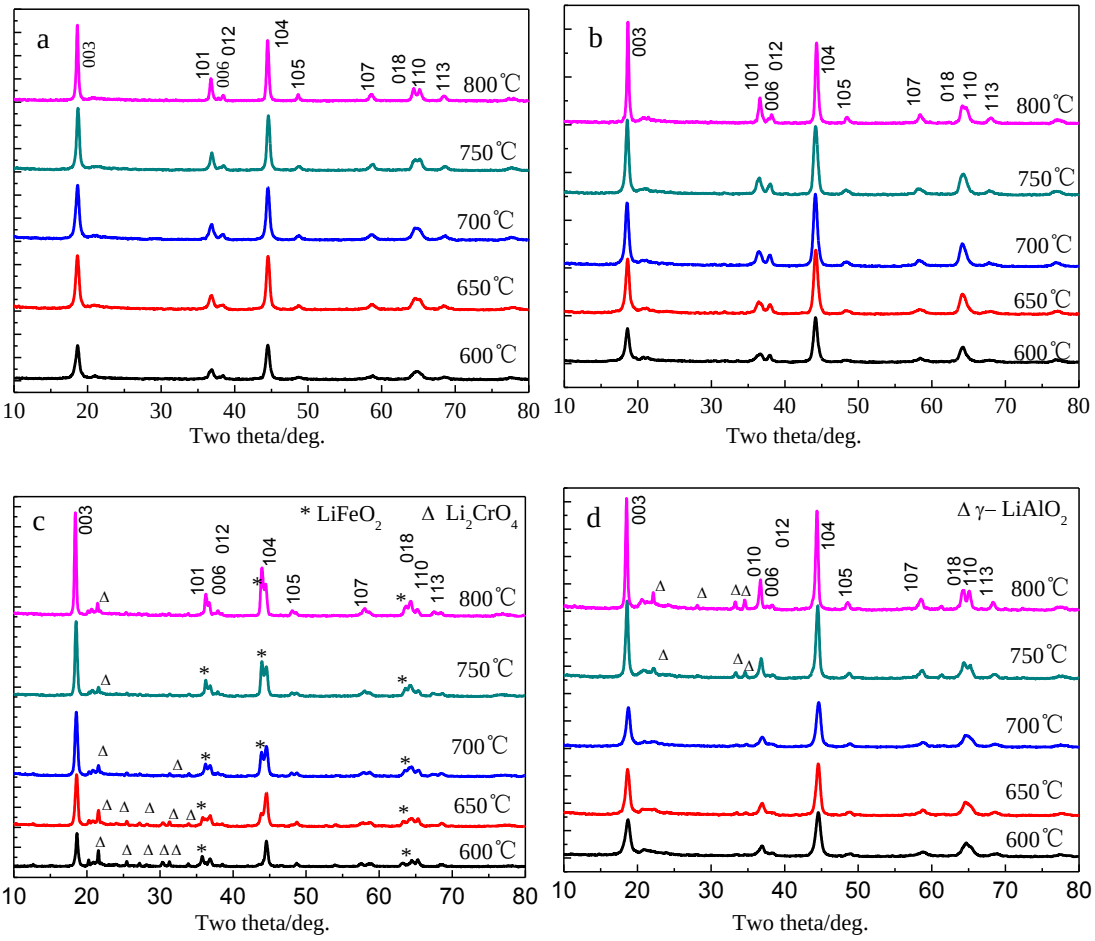

Figure 1. XRD patterns of Co-doped (a), Ni-doped (b), Cr-doped (c) and Al-doped (d) samples.

All of Co, Ni and Cr are multivalence metal ions. In order to clarify the valence, XPS analysis were carried out on as-prepared $Li(Li_{0.2}Mn_{0.4}Fe_{0.2}M_{0.2})O_2$ (M=Co, Ni, Cr) materials.

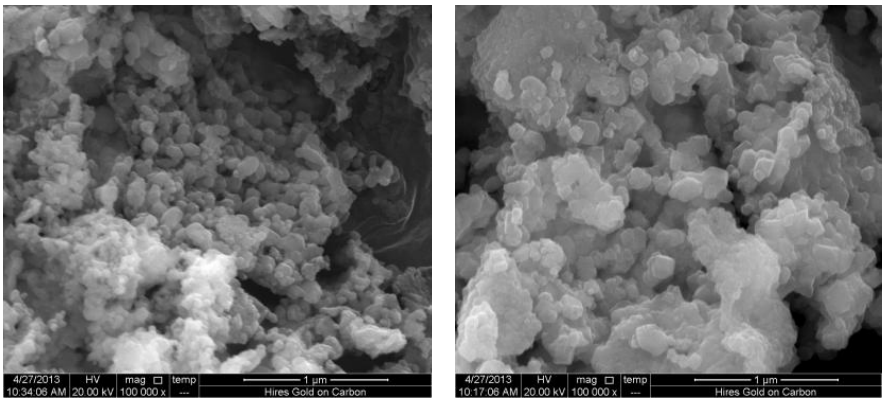

Co doping Ni doping

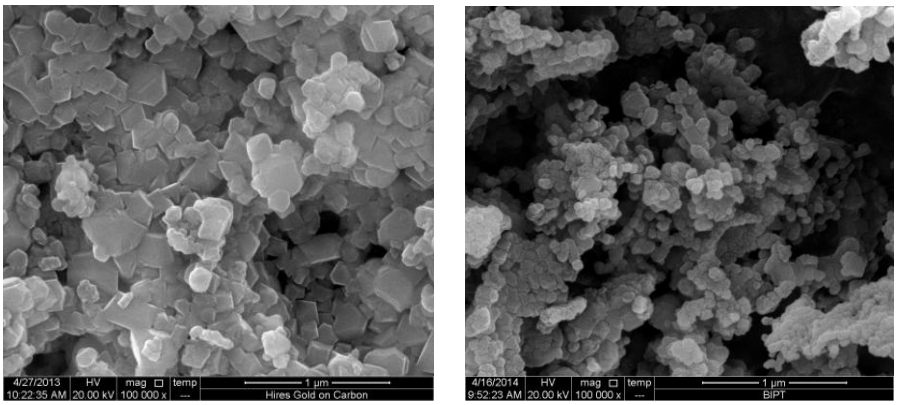

Figure 2. SEM images of $Li(Li_{0.2}Mn_{0.4}Fe_{0.2}M_{0.2})O_2$ (M=Co, Ni, Cr, Al) prepared at 700 ^oC.

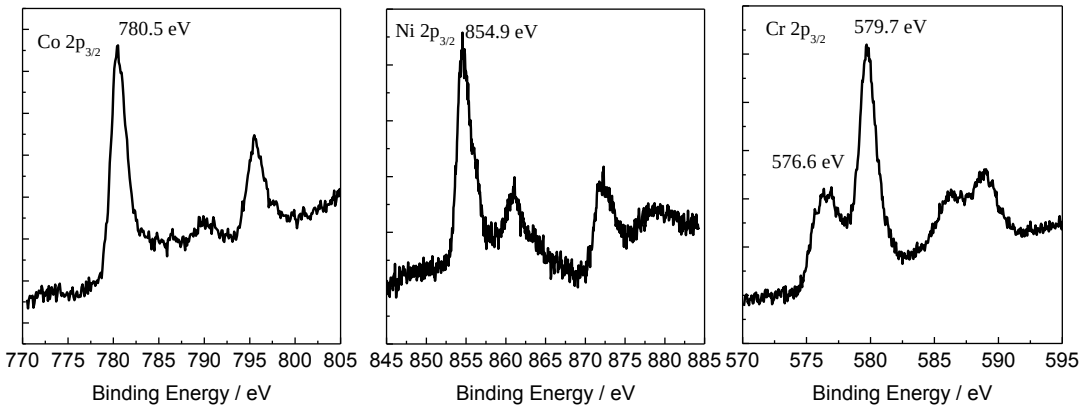

Figure 3. XPS patterns for cobalt ion, nickel ion and chromium ion in $Li(Li_{0.2}Mn_{0.4}Fe_{0.2}M_{0.2})O_2$ (M=Co, Ni, Cr).

Table I. The first discharge capacity of $Li(Li_{0.2}Mn_{0.4}Fe_{0.2}M_{0.2})O_2$ prepared at different temperature

	650 ^oC	700 ^oC	750 ^oC	800 ^oC
Capacity of S-Co / $mAhg^{-1}$	206.2	221.9	213.0	189.8
Capacity of S-Ni / $mAhg^{-1}$	192.6	211.0	193.9	176.2
Capacity of S-Cr / mAhg-1	128.4	155.2	134.5	134.5
Capacity of S-Al / $mAhg^{-1}$	158.6	183.7	146.6	122.3

Within this table, $Li(Li_{0.2}Mn_{0.4}Fe_{0.2}M_{0.2})O_2$ (M=Co, Ni, Cr, Al) samples are designated as S-Co, S-Ni, S-Cr and S-Al, respectively.

As shown in Fig.3, the Co $2p_{3/2}$ binding energy locates at 780.5 eV. This is consistent with that of Co^{3+} in CoOOH [28], confirming the +3 oxidation state of Co in the samples.

The Ni $2p_{3/2}$ binding energy of the samples center at 854.9 eV, which is a little smaller than that of Ni^{3+} in $LiNiO_2$ [29] but obvious higher than that of Ni^{2+} in NiO [30]。It indicates that nickel ions in the samples exist mainly in an oxidation state of Ni^{3+}. Small part of Ni^{2+} may come from NiO which has been reported to be formed on the surface of the nickel-containing metal oxides while stored in air

[31]. The Cr $2p_{3/2}$ peaks contain Cr^{3+} peak (CrOOH) at 576.6 eV and Cr^{6+} peak (CrO_3) at 579.7 eV [28], which further confirm that some chromium ions were oxidized to create Li_2CrO_4 impurity in $Li(Li_{0.2}Mn_{0.4}Fe_{0.2}Cr_{0.2})O_2$.

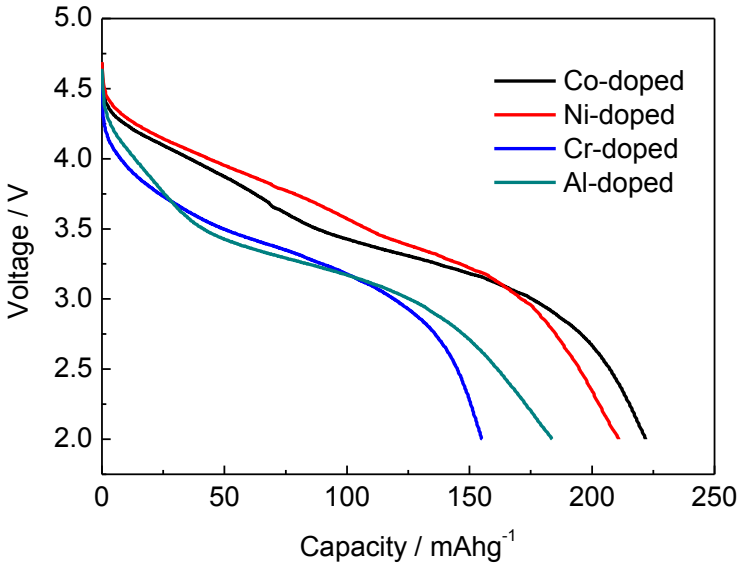

Figure 4. The first discharge curves of $Li(Li_{0.2}Mn_{0.4}Fe_{0.2}M_{0.2})O_2$ (M=Co, Ni, Cr, Al).

The first discharge capacities of as-prepared samples are presented in Table I. The samples prepared at 700 ^oC show higher capacity, which is same as $Li(Li_{0.23}Mn_{0.47}Fe_{0.2}Ni_{0.1})O_2$ [23]. Therefore, the samples prepared at 700 ^oC were chose to compare the electrochemical performance. The capacity of Cr-doped sample is close to that reported in literature [24], and such lower capacity can be attributed to the formation of Li_2CrO_4. Compared with Co- and Ni- doped samples, Al-doped sample also show a little lower capacity, which should be related to inactive Al^{3+}. Apart from the capacity, the shape of the first discharge curves is also remarkably different. As shown in Fig. 4, Ni-doped sample shows higher voltage plateau, but Al- and Cr- doped sample exhibits lower voltage plateau.

In order to further figure out the mechanism, cyclic voltammetry tests were carried out. As shown in Fig. 5, two oxidation peaks are observed below and above 4.4 V in the first charge curves. The oxidation peaks below 4.4 V have been attributed to Li extraction from $LiMO_2$ component accompanied by the reaction of Ni^{3+}/Ni^{4+}, Co^{3+}/Co^{4+} and Fe^{3+}/Fe^{4+} redox couple, and that above 4.4 V to an oxidation of O^{2-} ions and Li_2O extraction from Li_2MnO_3 component, respectively [5, 12-17, 25, 32]. Smaller oxidation peak below 4.4V can be observed for Cr- and Al- doped samples, which may be due to formation of Li_2CrO_4 and inactive Al^{3+}, respectively. In the process of discharge, two reduction peaks at ~3.1 V and ~3.8 V are observed. The peaks corresponding to the reduction of Co^{4+}, Ni^{4+} and Fe^{4+} mainly locate around 3.8 V, the peaks corresponding to the reduction reaction of Li-intercalation into MnO_2 formed after Li_2O removal from Li_2MnO_3 mainly locate around 3.4 V, and the reduction of Mn^{4+} in spinel $LiMn_2O_4$ to form $Li_{1+x}Mn_2O_4$ occurs at about 2.8V [23, 33, 34]. For Co-doped sample, two reduction peaks at ~3.1 V and ~3.8 V are obvious. Reduction voltage of ~3.1 V is higher than 2.8 V but lower than 3.4V, implying formation of some spinel-like phase. For Al-doped sample, there is

one small peak around 3.8V corresponding to the reduction of Fe^{4+}, and one large peak around 3.0 V corresponding to the reduction of Mn^{4+}.

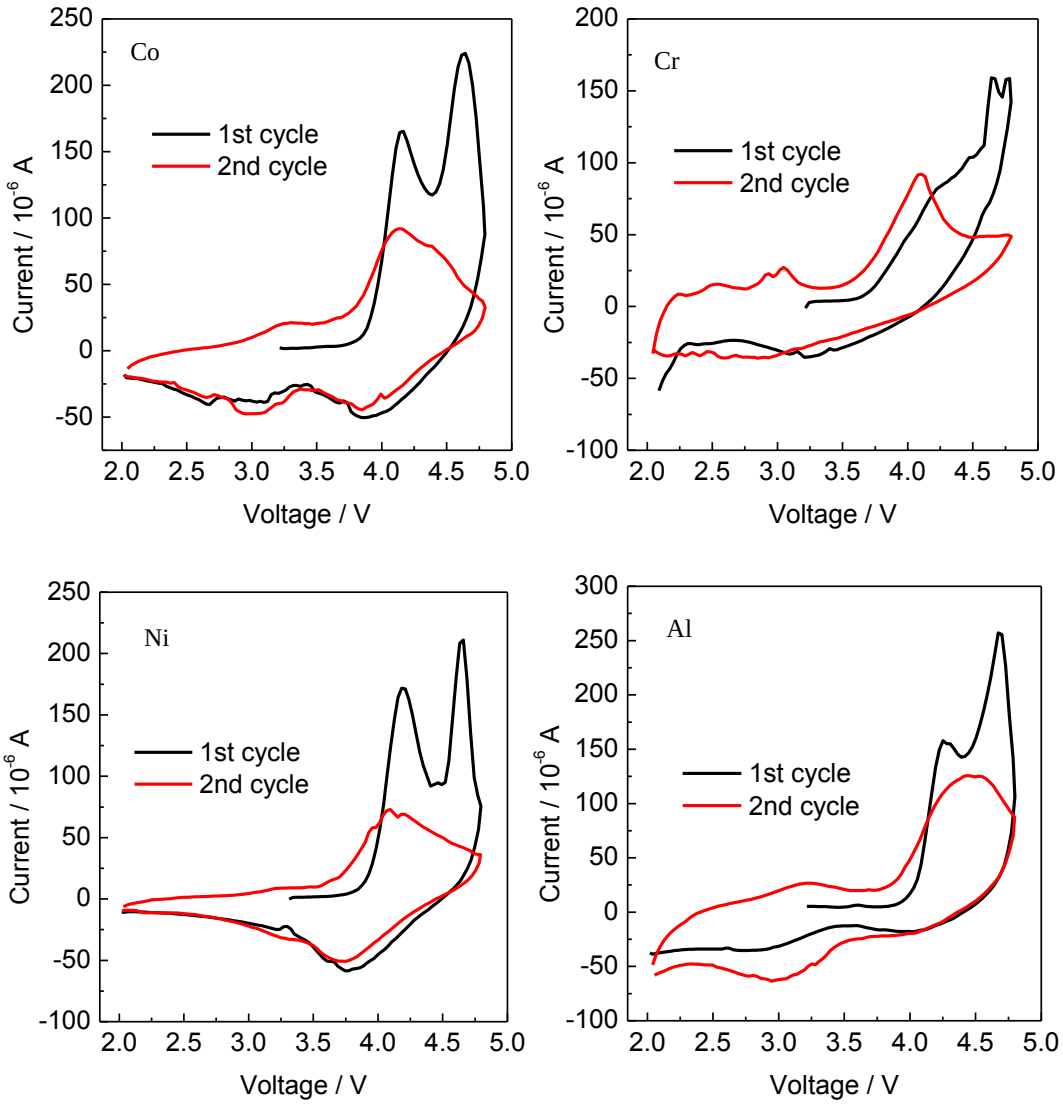

Figure 5. The cyclic voltammogram of $Li(Li_{0.2}Mn_{0.4}Fe_{0.2}M_{0.2})O_2$ (M=Co, Ni, Cr, Al).

However, only a small peak around 3.3V and a large peak around 3.7 V are observed in Ni-doped sample. Above results indicate that Ni-doping present remarkable effects on reducing structural transformation from layer to spinel-like for Li_2MnO_3-$LiFeO_2$ based materials. The discharge curves overlapped mainly in the second cycle for Co- and Ni- doped samples, indicating that the structure formed in the first discharge process is stable and reversible. The CV curves of Cr-doped sample are obvious different from the others, which may be attributed to Li_2CrO_4 phase.

The cycling performance of as-prepared materials are shown in Fig.6, The Co-, Ni, Cr- and Al-doped sample show an initial capacity of 221.9 $mAhg^{-1}$, 211.0 $mAhg^{-1}$, 155.2 $mAhg^{-1}$ and 183.7 $mAhg^{-1}$, and capacity retention of 86.7%, 86.3%, 86.7% and 83.1% after 21 cycles, respectively. According to Tabuchi et al. [15], the sample Y03 with the composition of $0.22LiFeO_2$-

$0.78Li[Li_{1/3}Mn_{2/3}]O_2$ can deliver a capacity of 233 $mAhg^{-1}$. However, its capacity declines to ~125 $mAhg^{-1}$, and its discharge voltage plateau also drop dramatically after 20 cycles.

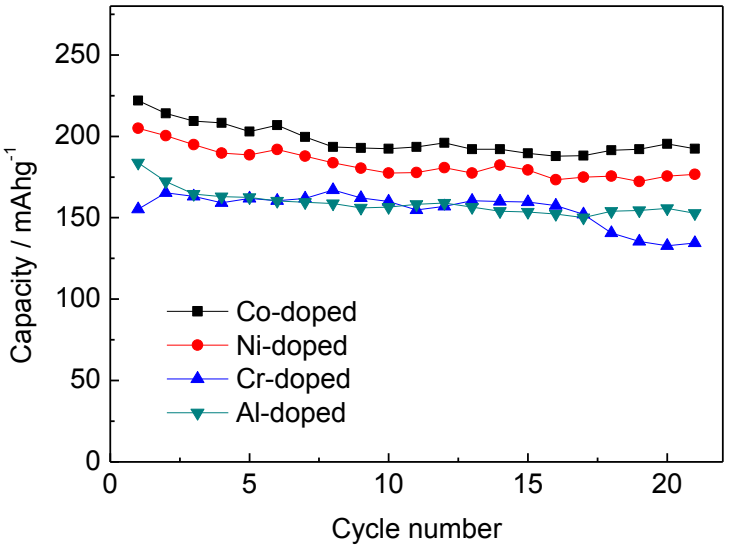

Figure 6. Cycling performance of $Li(Li_{0.2}Mn_{0.4}Fe_{0.2}M_{0.2})O_2$ (M=Co, Ni, Cr, Al).

Compared with sample Y03, $Li(Li_{0.2}Mn_{0.4}Fe_{0.2}M_{0.2})O_2$ (M=Co, Ni) show a little lower capacity, but remarkable improved cycling stability. It can be speculated that substitution of small portion of $Li[Li_{1/3}Mn_{2/3}]O_2$ in $LiFeO_2$-$Li[Li_{1/3}Mn_{2/3}]O_2$ solid solution by $LiNiO_2$ or $LiCoO_2$ may make great contribution to the improved cycleability. Compared with the Ni-doped Li_2MnO_3-$LiFeO_2$ based materials reported in literature [19], as-prepared $Li(Li_{0.2}Mn_{0.4}Fe_{0.2}Ni_{0.2})O_2$ in our work presents a close capacity but improved cycleability, which may be attributed to our proposed new preparation method [23]. Cr- and Al- doped sample show similar capacity retention, but their application is limited by both low capacity and voltage plateau. Such drawback may be reduced by decreasing the doped Cr- and Al- amounts. The studies on this issue are being carried out in our group.

4. CONCLUSIONS

All of Co- and Ni- doped samples prepared at 600 ^oC ~800 ^oC show pure layered α-$NaFeO_2$ phase. However, Al-doped sample with pure layered α-$NaFeO_2$ phase can only be obtained while annealed at 600 ^oC ~700 ^oC. In contrast, all of Cr-doped samples prepared at 600 ^oC ~800 ^oC contain impure phase of Li_2CrO_4 and $LiFeO_2$. All of doped samples annealed at 700 ^oC show the highest discharge capacity. Among them, both Co- and Ni- doped samples deliver higher capacity and voltage plateau, better structural stability during cycling. Compared with Co-doped sample, the Ni-doped sample show same capacity retention, a little lower capacity, but higher voltage plateau due to better reduction of the structural transformation from layer to spinel-like. Combined with the consideration of cost and toxicity, Ni doping is more promising. Cr doping is not beneficial to reducing the formation of

cubic $LiFeO_2$, both the capacity and voltage plateau are lower. For Al-doped sample, its capacity is a little lower due to inactive Al^{3+}, but its voltage plateau is also notable lower. In view of the good effects of inactive Al^{3+} on the structural stability, decreasing Al-doped amounts and co-doping with Ni or Co should be further investigated on modification of Li_2MnO_3-$LiFeO_2$ based materials in future.

ACKNOWLEDGMENTS

This work is supported by Beijing Natural Science Foundation (Grant No. 2122016), the MOST (Grant No. 2013CB934000, No. 2011CB935902, No. 2014DFG71590, No. 2013AA050903, No. 2011AA11A257 and No. 2011AA11A254), the Tsinghua University Initiative Scientific Research Program (Grant No. 2011THZ08139, No. 2011THZ01004 and No. 2012THZ08129) , Beijing Municipal Program (Grant No. YETP0157, No. Z131100003413002 and No. Z131100003413001) and State Key Laboratory of Automotive Safety and Energy (No. ZZ2012-011), Suzhou (Wujiang) Automotive Research Institute (Project No.2012WJ-A-01).

References

1. J.W. Fergus, *J. Power Sources* 195 (2010) 939.
2. Z. Lu, J.R. Dahn, *J. Electrochem. Soc*. 149 (2002) A1454.
3. C.W. Park, S.H. Kim, K.S. Nahm, H.T. Chung, Y.S. Lee, J.H. Lee, S. Boo, J. Kim, *J. Alloy Compds.* 449 (2008) 343.
4. J.-M. Kim, S. Tsuruta, N. Kumagai, *Electrochem. Comm*. 9 (2007) 103
5. M.M. Thackeray, S.H. Kang, C.S. Johnson, J.T. Vaughey, R. Benedeka, S.A. Hackney, *J. Mater. Chem.* 17 (2007) 3112.
6. Y. Sun, C. Ouyang, Z. Wang, X. Huang, L. Chen, *J. Electrochem. Soc*. 151 (2004) A504.
7. P.S. Whitfield, S. Niketic, I.J. Davidson, *J. Power Sources* 146 (2005) 617.
8. L. Zhang, K. Takada, N. Ohta, K. Fukuda, T. Sasaki, *J. Power Sources* 146 (2005) 598.
9. N. Yabuuchi, K. Yoshii, S.T. Myung, I. Nakai, S. Komaba, *J. Am. Chem. Soc*. 133 (2011) 4404.
10. J.-H. Lim, H. Bang, K.-S. Lee, K. Amine, Y.-K. Sun, *J. Power Sources* 189 (2009) 571.
11. Y. Wu, A. Manthiram, *Solid State Ionics* 180 (2009) 50–56.
12. M. Tabuchi, H. Shigemura, K. Ado, H. Kobayashi, H. Sakaebe, H. Kageyama, R. Kanno, *J. Power Sources* 97-98 (2001) 415.
13. M. Tabuchi, A. Nakashima, K. Ado, H. Sakaebe, H. Kobayashi, H. Kageyama, K. Tatsumi, Y. Kobayashi, S. Seki, A. Yamanaka, *J. Power Sources* 146 (2005) 287.
14. M. Tabuchi, A. Nakashima, K. Ado, H. Kageyama, and K. Tatsumi, *Chem. Mater*. 17 (2005) 4668.
15. M. Tabuchi, Y. Nabeshima, K. Ado, M. Shikano, H. Kageyama, K. Tatsumi, *J. Power Sources* 174 (2007) 554.
16. M. Tabuchi, Y. Nabeshima, T. Takeuchi, K. Tatsumi, J. Imaizumi, Y. Nitta, *J. Power Sources* 195 (2010) 834.
17. J. Kikkawa, T. Akita, M. Tabuchi, M. Shikano, K. Tatsumi, and M. Kohyama, *J. Appl. Phys*., 103 (2008) 104911.
18. M. Tabuchi, A. Nakashima, H. Shigemura, K. Ado, H. Kobayashi, H. Sakaebe, H. Kageyama, M. Kohzaki, A. Hirano, R. Kanno, *J. Electrochem. Soc*. 149 (2002) A509.
19. M. Tabuchi, Y. Nabeshima, T. Takeuchi, H. Kageyama, K. Tatsumi, J. Akimoto, H. Shibuya, J. Imaizumi, *J. Power Sources* 196 (2011) 3611.
20. K. Karthikeyan, S. Amaresh, G.W. Lee, V. Aravindana, H. Kim, K.S. Kang, W.S. Kim, Y.S. Lee, *Electrochim. Acta* 68 (2012) 246.
21. G. B. Liu, H. Liu, Y.F. Shi, *Electrochimica Acta* 88 (2013) 112.

22. X. Liu, T. Huang, A. Yu, *Electrochimica Acta* 133 (2014) 555.
23. J. Li, L. Wang, L. Wang, J. Luo, J. Gao, J. Li, J. Wang, X. He, G. Tian, S. Fan, *J. Power Sources* 244 (2013), 652.
24. T. Zhao, L. Li, S. Chen, R. Chen, X. Zhang, J. Lu, Feng Wu, K. Amine, *Journal of Power Sources* 245 (2014) 898.
25. A.R. Armstrong, M. Holzapfel, P. Novák, C.S. Johnson, S.H. Kang, M.M. Thackeray, P.G. Bruce, *J. Am. Chem. Soc.* 128 (2006) 8694.
26. Y. N. Ko, J. H. Kim, J. K. Lee, Y. C. Kang, J.-H. Lee, *Electrochimica Acta* 69(2012)345.
27. W. Liu, J. Gong, J. Yang, Z. Zong, G. Chen, Chemical Journal of Chinese University 26(2005)1484.
28. C. D. Wagner, W. M. Riggs, L. E. Davis, and J. Moulder, Handbook of X-ray photoelectron spectroscopy [M]. Minnesota: Perkin-Elmer Corp., 1992.
29. M.E. Spahr, P. Novak, B. Schnyder, O. Haas, R. Nespar, *J. Electrochem. Soc.* 145 (1998)1113.
30. S.H. Kang, J. Kim, M.E. Stoll, D. Abraham, Y.k. Sun, K. Amine, *J. Power Sources* 112 (2002) 41.
31. A.W. Moses, H.G.G. Flores, J.-G. Kim, M.A. Langell, *Applied Surface Science* 253 (2007) 4782.
32. Z. Lu, J.R. Dahn, *J. Electrochem. Soc.* 149 (2002) A815.
33. X.-J. Guo, Y.-X. Li, M. Zheng, J.-M. Zheng, J. Li, Zh.-L. Gong, Y. Yang, *J. Power Sources* 184 (2008) 414.
34. L. Yu, W. Qiu, F. Lian, J. Huang, X. Kang, *J. Alloy Compds*. 471 (2009) 317.